UNIVERSITY OF CALIFORNIA,
IRVINE

Expanding the Catalyst and Monomer Scope of Ring-Opening Polymerization-Induced Self-Assembly

THESIS

Submitted in partial satisfaction of the requirements for the degree of

MASTER OF SCIENCE

in Chemistry

by

Kyle Jacob Gassaway

Thesis Committee:
Assistant Professor Joe Patterson, Chair
Assistant Professor Seunghyun Sim
Professor Zhibin Guan

2023

DEDICATION

To

my parents, my siblings, and my coworkers

who saw my potential and pushed me to reach for it.

TABLE OF CONTENTS

LIST OF FIGURES

LIST OF TABLES

ACKNOWLEDGEMENTS

I would like to thank my committee chair, Professor Joe Patterson, for his dedication to educating the next generation of scholars. This dissertation would not have been possible without his guidance and persistent help.

I would also like to thank the members of my committee. Professor Zhibin Guan introduced me to research and UC Irvine, and Prof Seunghyun Sim introduced me to the field of polymers. Both scientists have had a tremendous impact on my career.

In addition, thank you to Dr. Paul Hurst for introducing me to ROPI-CDSA and for teaching me how to design experiments which further our knowledge of chemistry. Thank you to Paul Hurst, Jayme Chow, and Faris Abouchaleh for their help with cryoTEM, GPC, and MALDI-TOF data collection.

Financial Support was provided by the University of California, Irvine.

ABSTRACT OF THE THESIS

Expanding the Catalyst and Monomer Scope of Ring-Opening Polymerization-Induced Self-Assembly

by

Kyle Jacob Gassaway

Master of Science in Chemistry

University of California, Irvine, 2023

Assistant Professor Joe Patterson, Chair

Ring-Opening Polymerization-Induced Crystallization-Driven Self-Assembly (ROPI-CDSA) is a powerful method to create polymer nanoparticles for potential application in nanomedicine. In ROPI-CDSA, polyethylene glycol (PEG) is chain extended by the organocatalyzed ring-opening polymerization of L-lactide in toluene. Poly(L)-lactide (PLLA) is sparingly soluble in toluene, so the resulting PEG-*b*-PLLA block copolymers undergo self-assembly. For ROPI-CDSA to synthesize ideal drug delivery systems, it should utilize biocompatible components and be readily able to load drugs.

Current ROPI-CDSA approaches have used organocatalysts such as 1,5,7 triazabicyclodec-5-ene (TBD) to polymerize L-lactide onto PEG. TBD would need to be purified out before use in-vivo, and while PEG is biocompatible, there have been increasing reports of allergic reactions to PEG.[1] Here we show how chlorhexidine (Figure 1), an antibiotic[2], can act as a replacement catalyst for TBD and be incorporated into the self-assemblies without a separate drug-loading step, and how the more biocompatible and versatile poly-2-ethoxy-2-oxo-1,3,2-dioxaphospholane (PEP) can act as a replacement for PEG.[3]

These studies lay the framework for new drug delivery systems. In future studies, different drugs bearing the proper functional groups can substitute for chlorhexidine. The incorporation of phosphoesters in ROPI-CDSA, such as PEP, will allow for increasing synthetic versatility as phosphoesters with different side chains can be utilized in future studies.[3] Thus, the synthetic development of chlorhexidine-catalyzed ROPI-CDSA and the use of PEP in ROPI- CDSA, are the first steps towards new ROPI-CDSA drug delivery systems.

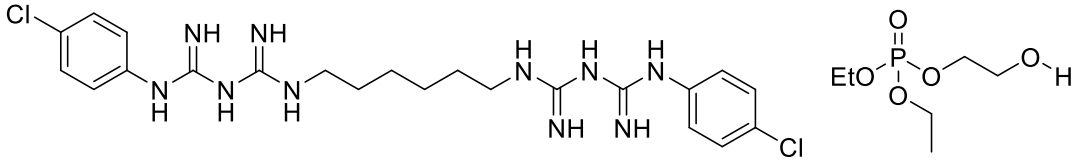

Figure 1: *Chlorhexidine (left) is an antibiotic which contains bisguanidine groups. These functional groups make the pharmaceutical a candidate for ring-opening polymerization catalysis. PEP (right) is a biocompatible polymer which could potentially replace PEG*

INTRODUCTION

Materials are often discussed in terms of molecular properties and bulk properties, but the nanoscale is a versatile domain for tuning the properties of materials. Polymers can assemble together into micelles, rods, vesicles, and other morphologies for a wide variety of applications.[4,5,6] Polymer-based nanoparticles are already used in lubricants, drug-delivery systems, biosensors, nanoreactors, and many more products.[7,8] Polymer nanoparticles are often made from self-assembled block copolymers.[4]

Block copolymers (BCPs) are polymers which contain two or more distinct sections, or "blocks" made from different monomers. If one block is soluble in a solvent (solvophilic) but the other is insoluble (solvophobic), then the BCPs may spontaneously self-assemble into nanoparticles to minimize the unfavorable interactions between the solvophobic block and the solvent.[4] When these nanostructures form under thermodynamic control, the morphology can often be predicted by the packing parameter P, the ratio of the volume occupied by the solvophobic block to the solvophilic block.[9] If $P < 1/3$, then the solvophilic block will fully encapsulate the solvophobic block in a sphere, but if $P > 1$, then the solvophobic block will be too large to encapsulate. Between 1/3 and 1, different nanoparticle morphologies will form, such as cylinders and vesicles.[9]

Some methods, however, produce nanoparticle morphologies which aren't predicted by this simple relationship. If the exchange rate of BCPs between nanoparticles is very slow or non-existent, then the BCPs may form kinetically trapped morphologies. These "non-ergodic"[10] structures may not follow the trend outlined above. The final morphology may depend on the temperature or the initial concentration of the reagents.[10]

Two common techniques for self-assembling BCPs into nanostructures are direct dissolution and solvent-switch. In direct dissolution, dry BCP is directly added to a solvent which will trigger self-assembly upon dissolution.[11] In solvent-switch, the BCP is dissolved in a solvent in which it is completely soluble (e.g. a water-miscible organic solvent), and then a second solvent (e.g. water) is added which will trigger self-assembly.[12] Although popular, both methods usually produce low concentrations of nanoparticles, which makes synthesis difficult to scale for industrial purposes.[4]

To address the scalability of BCP self-assembly, polymerization-induced self-assembly (PISA) has been developed as a one-pot technique to synthesize and assemble BCPs. In PISA, a solvophilic block is chain extended with a monomer that forms a solvophobic block. As the polymerization progresses, the growing BCP will self-assemble. This technique can be used to form complex nanostructure morphologies, such as worms, vesicles, and lamellae.[4] PISA can be used to produce nanostructure solutions of up to 50% wt.,[13] and many different methods have been explored to initiate PISA, including reversible addition–fragmentation chain transfer (RAFT) and ring-opening metathesis polymerization (ROMP).[14,15]

Although PISA is versatile and scalable, it's often difficult to produce anisotropic structures such as worms and lamella. Crystallization-driven self-assembly (CDSA) is a self-assembly technique which addresses this issue.[16] For this technique, the solvophobic, "core-forming" block is made from a polymer which will crystallize, as opposed to the amorphous cores in PISA-formed nanoparticles. The polymers are heated, then cooled in a solution, similar to single-solvent recrystallization. The solvent used will solubilize both polymer blocks when warm, but only the solvophilic block when cool. CDSA can access a wide range of morphologies through varying the size of the polymer blocks and the initial conditions of the self-assembly.[10,17] Poly-L-

lactide (PLLA) is the crystallizing core block[18] which regulates the size and morphologies of the nanoparticles described in this dissertation. L-lactide is a cyclic monomer which can be polymerized by releasing the potential energy stored in the ring strain.

Ring-opening polymerization (ROP) is an efficient and effective technique for polymerizing cyclic esters, such as L-lactide[4,19]. A base can be used as a catalyst to open the ring, then an initiator, such as methyl polyethylene glycol (mPEG) attacks the modified monomer and extends the polymer into a new initiating intermediate[20] (Schemes 1 and 2).

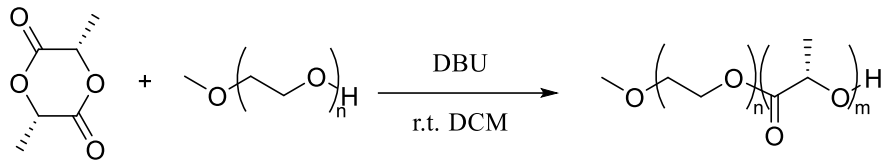

Scheme 1: *Synthesis of PEG-b-PLLA using DBU as a catalyst.*

Diazabicyclo(5,4,0)undec-7-ene (DBU) and 1,5,7 triazabicyclodec-5-ene (TBD) are established catalysts which can open L-lactide and form PEG-*b*-PLLA.[20,21] As the polymers grow, PLLA becomes less soluble in toluene[22,23] and begins to crystalize. The BCPs then self-assemble into kinetically trapped spheres, rods, vesicles, or lamellae.[19,24] This hybrid approach to forming nanoparticles is called ring-opening polymerization-induced crystallization-driven self-assembly (ROPI-CDSA).

ROPI-CDSA is a powerful combinate of PISA and CDSA for creating anisotropic nanoparticles in solution which could find future application in drug delivery. To expand the scope and increase the application potential of ROPI-CDSA, this dissertation explores the use of chlorhexidine, an antibiotic,[2] as a new catalyst and PEP as a new solvophilic corona. Chlorhexidine contains guanidine groups similar to TBD, which makes the pharmaceutical a good candidate for ROP catalysis. If chlorhexidine is incorporated into the resulting nanostructures, it could be used to make application-ready drug delivery systems. When L-lactide is added to mPEG in the

presence of chlorhexidine, it polymerizes into PEG-*b*-PLLA. It was also found that L-lactide will polymerize into PLLA if polyethylene glycol dimethyl ether (m_2PEG) is used instead of mPEG. m_2PEG is a polymer similar in structure to mPEG, but it lacks the alcohol group needed to initiate ROP. This finding suggests that chlorhexidine acts as an initiator, as well as a catalyst (Figure 2).

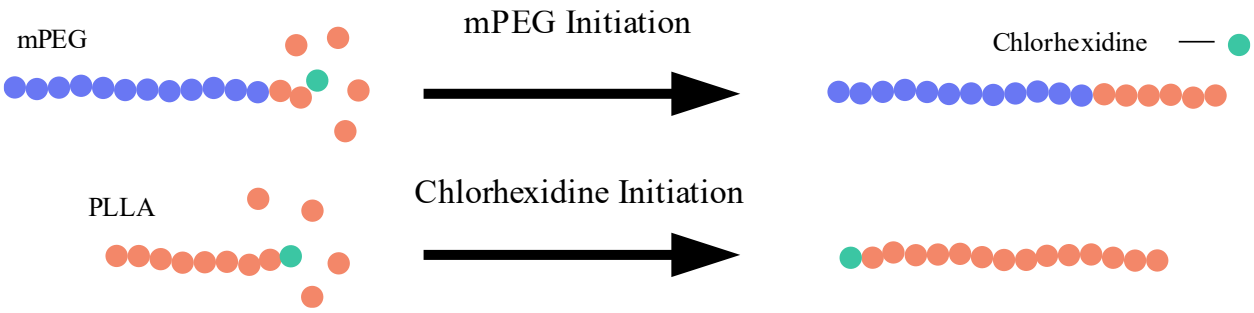

Figure 2: *mPEG (blue) will initiate the polymerization of L-lactide (red), and chlorhexidine (green) will catalyze the polymerization to form PEG-b-PLLA (top). In the absence of mPEG, chlorhexidine polymerizes L-lactide into PLLA, which suggests that chlorhexidine initiates the polymerization (bottom).*

Although PEG is used in many biomedical applications, it does not degrade in the body well, and it can cause allergic reacitons.[1,3] Polyphosphates have promising biocompatibility, and feature a customizable side-chain, which makes them attractive alternatives to PEG for the solvophilic block.[3] 2-Ethoxy-2-oxo-1,3,2-dioxaphospholane (EP) is a cyclic monomer which can be polymerized through many of the same catalysts as L-lactide.[25] Here, poly-ethoxy-2-oxo-1,3,2-dioxaphospholane (block) poly-L-lactide (PEP-b-PLLA) is synthesized in a one-pot, two-step system (Scheme 2), and the subsequent BCPs self-assemble in toluene.

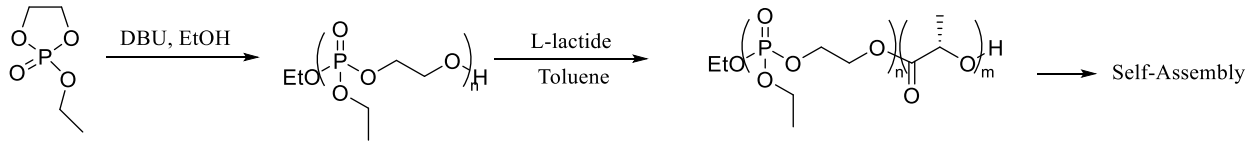

Scheme 2: *Synthesis of PEP-b-PLLA through a one-pot, two step synthesis.*

RESULTS AND DISCUSSION

1 CHLORHEXIDINE-CATALYZED PEG-*b*-PLLA SELF-ASSEMBLY

1.1 CHLORHEXIDINE AS A CATALYST

To investigate the use of chlorhexidine as a catalyst for ROPI-CDSA, DBU, an established ROP catalyst[21,26], was used to synthesize PEG-*b*-PLLA in DCM for comparison to the BCPs catalyzed by chlorhexidine (Table 1). The synthesis procedure is outlined by Lohmeijer et al.,[21] and the BCPs were characterized using proton Nuclear Magnetic Resonance spectrometry (^{1}H NMR). The hydrogen peaks produced by the backbone of the PLLA chain are resolvable from the peaks produced by hydrogen atoms in the L-lactide monomers, so it is possible to determine the ratio of polymerized L-lactide monomers to closed (unpolymerized) L-lactide monomers through ^{1}H NMR. This ratio was used to calculate percent conversion (Table 1). The BCPs were purified using diethyl ether and analyzed using ^{1}H NMR and Gel Permeation Chromatography (GPC). The signal created by the end group (Figure 3) is relatively low compared to the signals created by the polymer backbone, but the signal created by the pre-polymerized mPEG backbone is a reliable standard for calculating the degree of polymerization. The dispersity of the BCPs was determined using GPC; the elution curves for each BCP were fitted to a calibration curve (Figure 4). The dispersities were found to range from 1.22 to 1.81. One hypothesis for this is that chlorhexidine initiates polymerization as well as catalyzes it. If this hypothesis were correct, it would be expected that the GPC would likely have two peaks, but this was not seen.

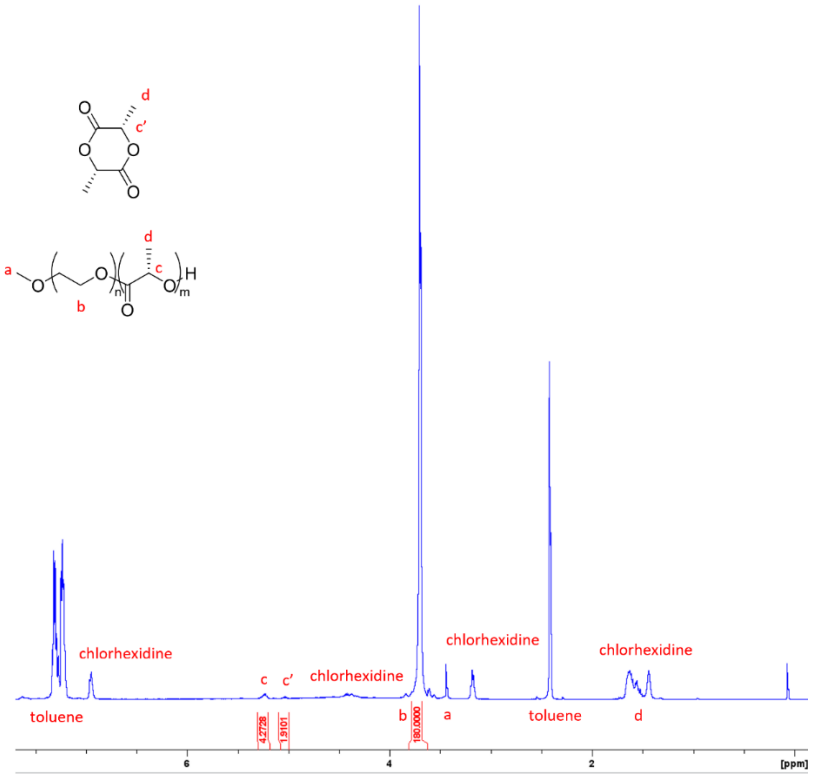

Figure 3: *Representative crude ^{1}H NMR of PEG-b-PLLA after chlorhexidine ROP. % Conversion was calculated by dividing the area under peak c by the sum of peaks c and c'. See Figure S1 for labeling of chlorhexidine peaks.*

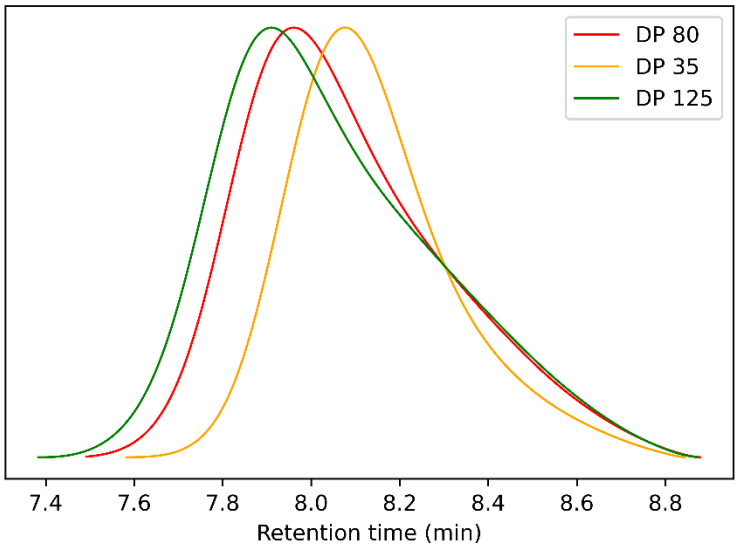

Figure 4: *GPC retention time of chlorhexidine-catalyzed ROP (Polymers 2,3 and 4 in Table 1). Polydispersity was calculated using a polystyrene calibration curve.*

After the data were obtained for PEG-b-PLLA BCPs made using DBU, BCPs were synthesized using chlorhexidine as the catalyst (Scheme 3). We tested the polymerization reaction using different amounts of chlorhexidine, and 5% mol. chlorhexidine yielded greater than 90% conversion for PEG-b-PLLA$_{45}$ and PEG-b-PLLA$_{90}$, so this ratio was used to polymerize BCPs comparable in molecular weight to the BCPs made using DBU. These BCPs were synthesized in toluene, rather than DCM, to allow the BCPs to self-assemble as polymerization occurred. The mPEG assists in dissolving the chlorhexidine, which otherwise is not very soluble in toluene.

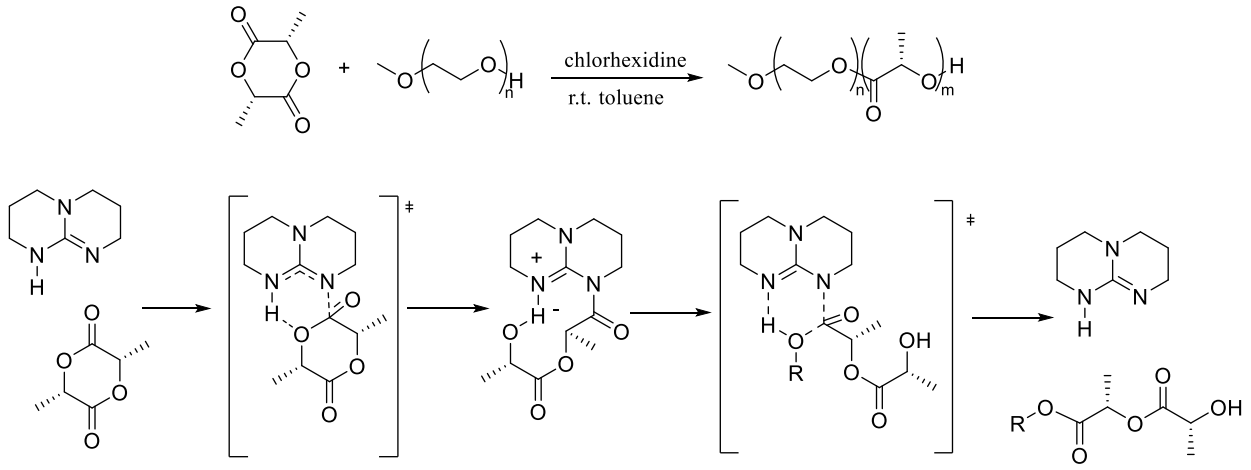

Scheme 3: *PEG-b-PLLA can be synthesized using chlorhexidine as a catalyst (top), generating application-ready self-assemblies. Chlorhexidine contains guanidine groups and likely goes through a similar catalytic mechanism to the one depicted for TBD[20] (bottom)*

Many of the BCP samples became turbid in toluene, indicating the presence of nanoparticles, and cryo Transmission Electron Microscopy (cryoTEM) analysis revealed the formation of lamellae, nanorods, and vesicles (Figure 5). The target Degree of Polymerization (DP) and the weight % of the reagents both affected the dominant morphology. If the PLLA chain occupies roughly the same volume as the mPEG chain (P ≈ 1), then mPEG chain will tend to sandwich the PLLA into flat lamellae. High-curvature nanoparticles, such as spheres and rods, preferentially form when the PLLA chain is much shorter and more compact than the mPEG chain.[27] These rods may aggregate into lamellae under high concentrations if kinetically rapid.[19]

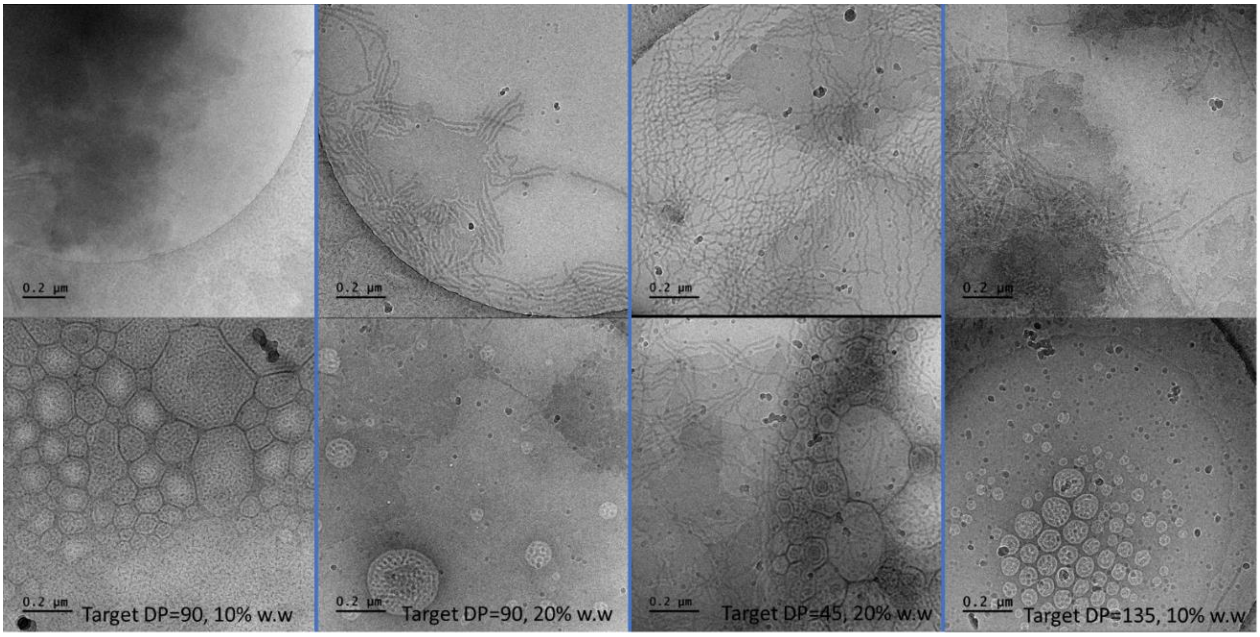

Figure 5: *When chlorhexidine catalyzes the ROP of PEG-b-PLLA, the BCPs self-assemble into rods, vesicles, and compound vesicles, depending on the concentration and target DP. Reactions 1, 3, & 4 (left to right) and all cryoTEM images were run and collected by Paul Hurst.*

^{1}H NMR confirmed that chlorhexidine can be used to effectively to polymerize L-lactide with high conversion (Table 1), except when a very low amount of L-lactide is used. Chlorhexidine can also synthesize PEG-*b*-PLLA reliably, except when the ratio of L-lactide is very high; conditions which should have yielded PEG_{45}-*b*-$PLLA_{200}$ instead appeared to yield PEG_{45}-*b*-$PLLA_{150}$ and PEG_{45}-*b*-$PLLA_{170}$.

The difference between the actual degree of polymerization and the target degree of polymerization for larger polymers (Table 1) supports the hypothesis that chlorhexidine can co-initiate ROP. The mPEG likely out-competes chlorhexidine initiation, which is why the short-chain BCPs readily form. The high abundance of L-lactide in longer BCPs likely thermodynamically pushes chlorhexidine initiation forward, creating PLLA homopolymers. This side reaction explains why the conversion of L-lactide to PLLA is still high for larger BCPs, even though the actual degree of polymerization is much lower than the target.

Table 1: Characterization of PEG-*b*-PLLA block copolymers made via ROP

BCP	Catalyst	Weight %	% Conversion	Degree of Polymerization (DP)	Target DP
1	Chlorhexidine	8	70	4	5
2	Chlorhexidine	20	>95	35	35
3	Chlorhexidine	20	>95	80	90
4	Chlorhexidine	20	>95	125	135
5	Chlorhexidine	10	>95	170	200
6	Chlorhexidine	20	>95	150	200
7	DBU	7	>98	50	50
8	DBU	6	>98	105	100
9	DBU	5	>98	155	150
10	DBU	5	>98	200	200

1.2 CHLORHEXIDINE AS AN INITIATOR

To test whether chlorhexidine can act as an initiator as well as a catalyst (Scheme 4), the chlorhexidine-catalyzed ROP conditions were repeated, but polyethylene glycol dimethyl ether (m_2PEG) was substituted for mPEG. Unlike mPEG, m_2PEG is methylated at both ends and therefore cannot initiate ROP. However, the polymer is similar enough to mPEG to assist in solubilizing chlorhexidine in toluene, so it acts as an appropriate control.

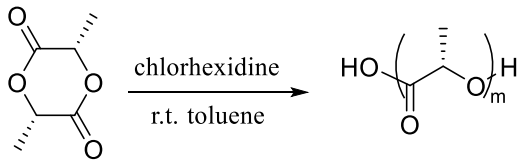

Scheme 4*: Chlorhexidine can also be used to initiate ROP of L-lactide, producing PLLA homopolymers*

The products were isolated and found to contain PLLA, as determined by ^{1}H NMR (Figure 6). The % conversions were not as high as mPEG-initiated ROP for short-chain polymers (*PEG-b-PLLA*$_{45}$), but they were comparable for mid-chain polymers (*PEG-b-PLLA*$_{135}$), especially in more concentrated solutions.

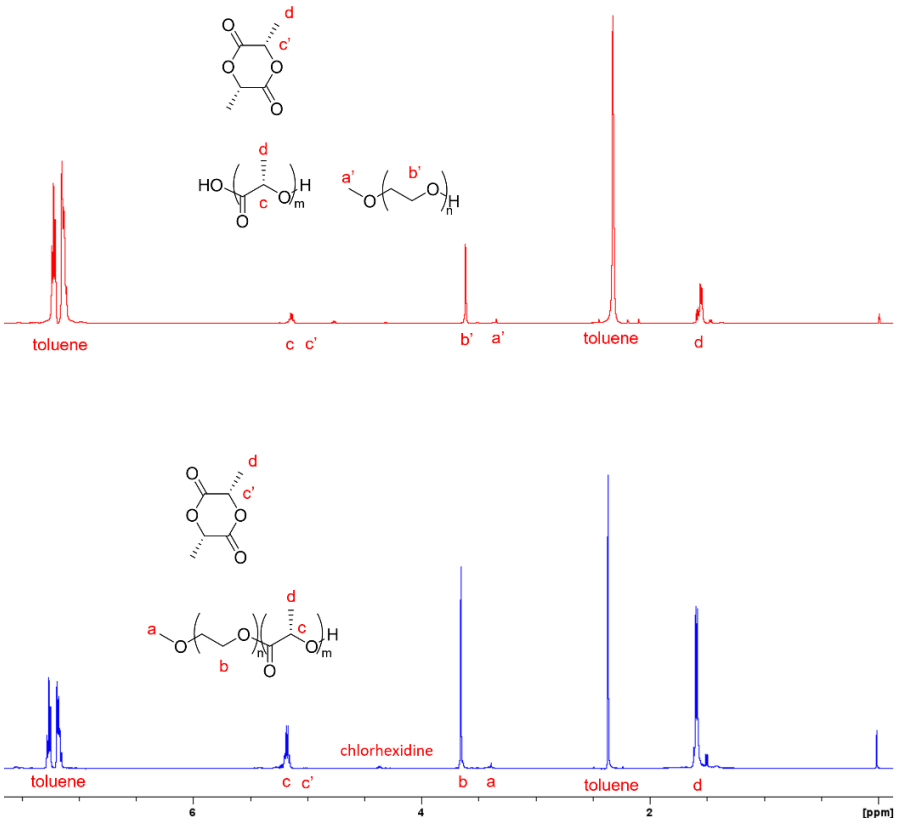

Figure 6: *Representative crude ^{1}H NMRs of PLLA ROP initiated with chlorhexidine (above) and mPEG (below). The peaks at 5.18 ppm (c) indicate that both conditions result in the polymerization of L-lactide.*

Table 2: Characterization of PLLA homopolymers initiated by guanidine-containing catalysts

Polymer	Initiator/Catalyst	Wt %	% Conversion	Target DP*
1	Chlorhexidine	20	90	90
2	Chlorhexidine	20	80	135
3	TBD	20	7	90
4	TBD	20	10	135

**In this table, "% Conversion" is the percent of L-lactide converted to PLLA as calculated by ^{1}H NMR, and the "Target DP" is the degree of polymerization expected for PLLA under the reaction conditions if mPEG were used instead of m_2PEG*

To fully characterize the homopolymers, it is necessary to determine whether the chlorhexidine remains bound to the PLLA, or whether trace mPEG was generated from the m_2PEG and is bound to the PLLA. While ^{1}H NMR data are useful in quantifying the amount of L-lactide opened by the reaction (Figure 6), they cannot be used to determine if m_2PEG or chlorhexidine is bound to the homopolymers.

To further characterize the chlorhexidine, we prepared and processed FTIR samples of the polymers and of chlorohexidine to look for modifications to the chlorhexidine. Chlorhexidine produces a broad FTIR peak at ~1670 cm^{-1}, which likely correlates to the C=N bond in the guanidine group[28,29], but this peak is not present in PEG-*b*-PLLA (Figure 7 a). The crude product did not contain this peak, even though a chlorhexidine peak at ~1610 cm^{-1} was still present. These data indicate that chlorhexidine is modified during the reaction.

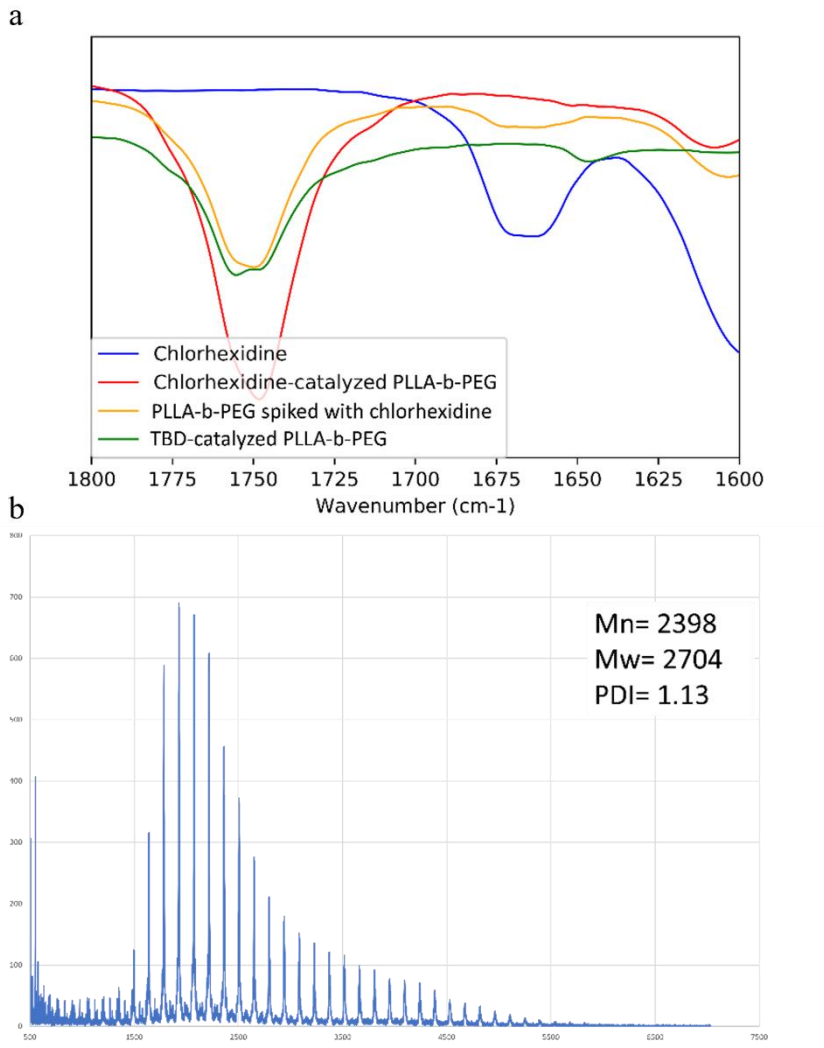

Figure 7: *(a) FTIR data collected on chlorhexidine before and after ROP (left). The peak at 1670 cm^{-1} likely correlates to the C=N bond in the guanidine group[28,29]. The disappearance of the peak indicates that chlorhexidine is modified by the reaction. These data were collected by Paul Hurst and me. (b) MALDI-TOF data for the chlorhexidine-initiated homopolymer (right) contains the*

triplet peaks which indicate the presence of chlorhexidine. These data were collected by Faris Abouchaleh.

Normally, an initiator stays bound to the extending polymer, like mPEG, and analysis with MALDI indicates that this is the case for chlorhexidine (Figure 7 b). Faris Abouchaleh, an undergraduate in the Patterson lab, prepared and processed MALDI-TOF samples for the homopolymers, and it was determined that PLLA polymers exist in the solution independent of the m_2PEG, as expected. It was also determined that chlorhexidine is bound to the homopolymers. Chlorhexidine contains two chlorine atoms, and chlorine consists of two primary isotopes, ^{37}Cl and ^{35}Cl, with relative abundances of 24% and 76% respectively. With two isotopes and two chlorine atoms per chlorhexidine, four isotope peaks were observed, which supports the conclusion that chlorhexidine initiates the ROP of L-lactide and is modified by the initiation, and it becomes chemically bound to final homopolymer.

2 TWO-STEP PEP-*b*-PLLA SELF ASSEMBLY

Although PEG is a popular polymer for biomedical applications, it's not the most biocompatible polymer; it doesn't degrade well in biological conditions. Polyphosphates such as PEP show promise for being more biocompatible than PEG, which would be ideal in a drug delivery system.[3] To test the viability of PEP-b-PLLA self-assemblies, PEP-b-PLLA BCPs were prepared in toluene and characterized with cryoTEM.

2.1 CATALYST OPTIMIZATION

EP and L-lactide can be polymerized using many of the same ROP catalysts.[25] Ideally, EP could be polymerized in the bulk, then L-lactide and toluene could be added to the solution in a one-pot, two-step synthesis (Scheme 2). In order to reduce the variables in self-assembly, it's necessary to synthesize uniform BCPs with low polydispersity through controlled polymerization.

Procedures for the polymerization of EP were adapted from Clément et al.[25] and Lim et al.[30] TBD was first used to synthesize PEP-b-PLLA, but the catalyst yielded BCPs with broad dispersity in two resolvable size distributions (Figure 8). Although TBD has been used to successfully synthesize PEP,[25] it's possible that the short PEP chain lengths in this application lead to a high dispersity of 2.37 through chain-fusion events due to undesirable trans-esterification reactions. DBU was used in place to TBD and yielded BCPs with much lower dispersity of 1.25 through a more controlled reaction. DBU was therefore used in subsequent synthesis reactions.

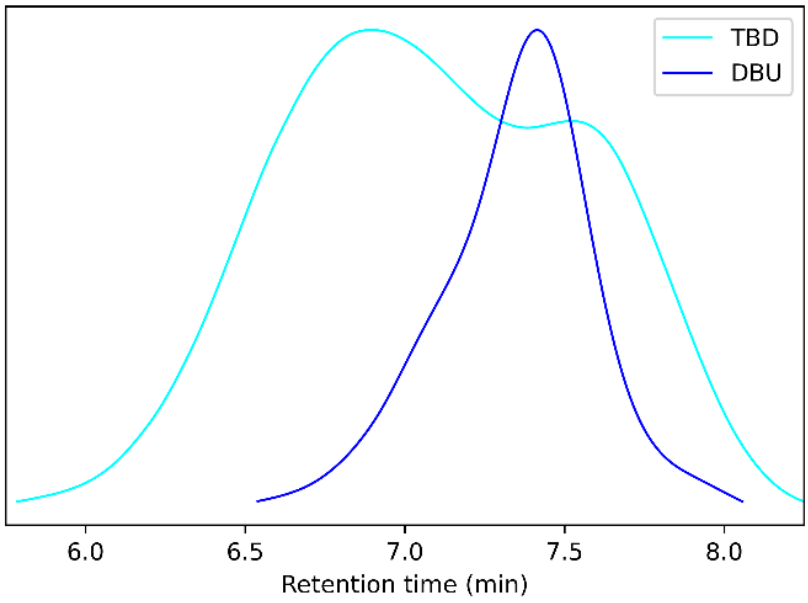

Figure 8: *GPC retention time of TBD and DBU-catalyzed PEP-b-PLLA BPCs. Polydispersity was calculated using a polystyrene calibration curve.*

2.2 POLYPHOSPHATE CHARACTERIZATION

The self-assembly is driven by the amphiphilic nature of the BCPs,[9] so it's important that the PEP forms a solvophilic block distinct from the solvophobic PLLA block. When two cyclic monomers are introduced to a ROP catalyst, the fastest-propagating monomer often polymerizes first and begins to transesterify before the slower-propagating monomer is incorporated (if it opens at all).

A common way to make block copolymers which share a ring-opening organocatalyst is to introduce the slower-propagating block first, then to add the faster-propagating monomer once the first block has formed.[31] To ensure that the EP monomer polymerizes before the addition of the L-lactide, PEP polymerization reactions were quenched with benzoic acid and the products were characterized through GPC and MALDI-TOF MS (Figure 9**)**. GPC analysis confirmed the presence of molecules in the solutions larger than the monomer with low dispersities of 1.07 and 1.03 for PEP chain lengths of 5 and 10 respectively. MS analysis revealed peaks separated by 152 g/mol, the mass of the monomer, which confirmed the presence of polymers.

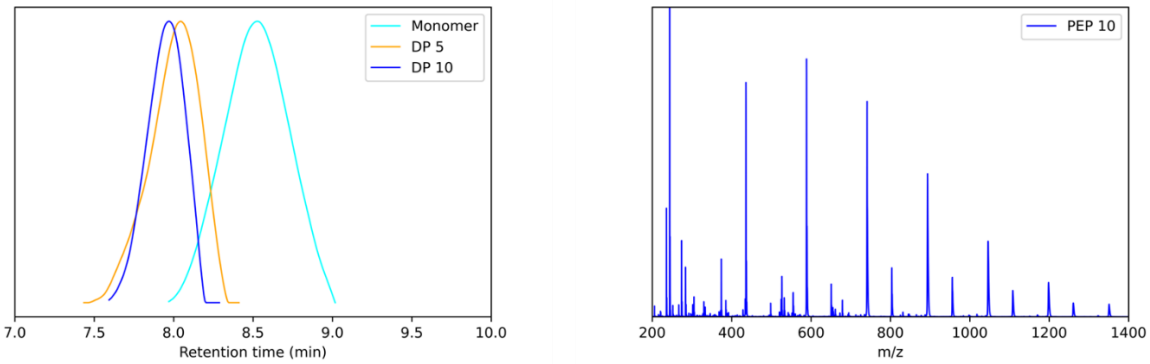

Figure 9: *GPC and MALDI-TOF MS data confirm the presence of PEP homopolymers before L-lactide is added to the solution. Data collected with help from Faris Abouchaleh and Jayme Chow.*

2.3 PEP-b-PLLA SELF-ASSEMBLY

Once the catalyst was optimized and the presence of PEP blocks was confirmed, the self-assemblies of the BCPs were characterized. After polymerization, many samples turned turbid, which indicates the presence of particles large enough to scatter light (Table 3).

Table 3: *Characterization of PEP-*b*-PLLA BCPs in toluene

PEP DP	PLLA DP	Wt %	Turbid?	% Conversion	Đ
10	50	30	Y	96.5	1.17
10	100	20	Y	95.6	1.19
10	100	5	Y	95.0	1.33
20	150	20	Y	95.8	1.38

*See Table S1 for a full list of BCP lengths and initial concentrations

The turbidity of the samples depends on the lengths of the PEP block and the PLLA block, and on the concentration of the solids at the time of self-assembly (Figure 10). The trend in turbidity is especially significant because it means that the initial reaction conditions affect the ending state of the system, even if the final BCPs are the same size. In other words, it is strong evidence that the final state of the system is path dependent.[19]

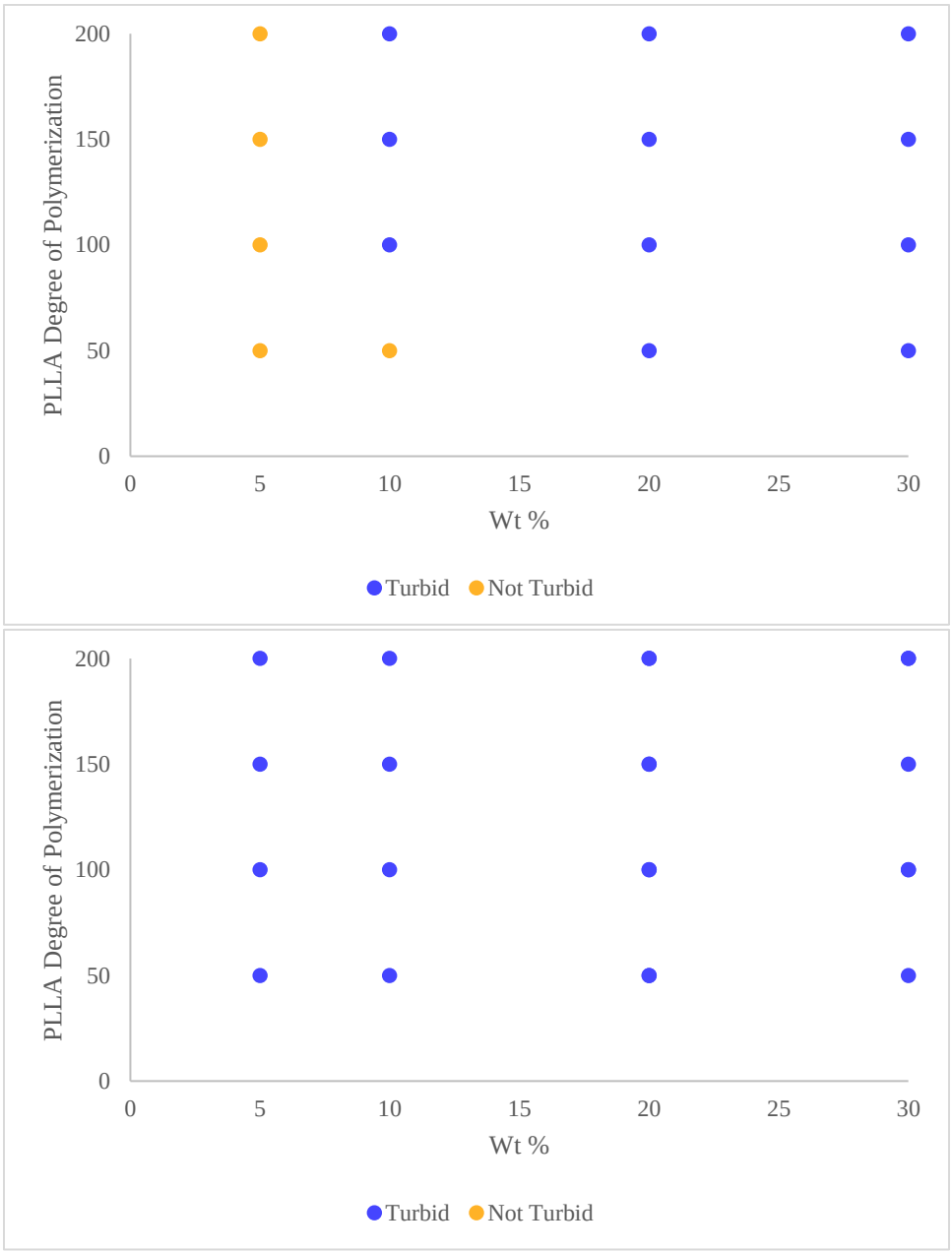

Figure 10: *The turbidity of PEP_{20}-b-$PLLA_n$ (top) and PEP_{10}-b-$PLLA_n$ (bottom) BCPs prepared in toluene. The turbidity of the final BCP solution depends on the lengths of both polymer blocks and the BCP concentration at the time of L-lactide polymerization.*

A sample of PEP_{10}-b-$PLLA_{50}$ was resuspended in water and characterized using cryoTEM and found to contain nanofibers (Figure 11). The anisotropic nature of the fibers is a strong indication that the L-lactide blocks in the center of the fibers are semi-crystalline. Dry cryoTEM was performed on a sample of BCPs of the same length, prepared at a different concentration, and the sample was found to contain aggregates of lamellae (Figure 12). The final length of the BCPs was the same, but the morphology depended on the initial concentration of the reagents, which indicates that the formation of the self-assemblies is path dependent.

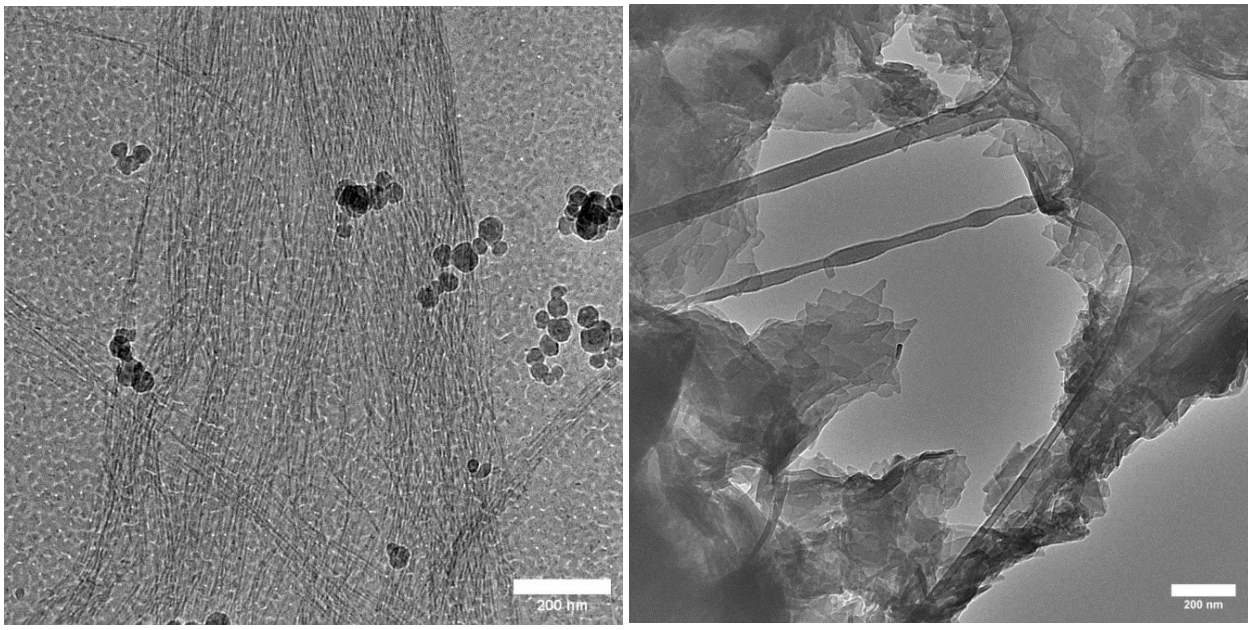

Figure 11: *(left) CryoTEM image of PEP_{10}-b-$PLLA_{50}$ nanofibers and ice crystals (black), (right) dry cryoTEM image of PEP_{10}-b-$PLLA_{150}$ lamellae aggregates. Different BCP lengths and concentrations result in fibers, lamellae, and other morphologies (Figure S 4).*

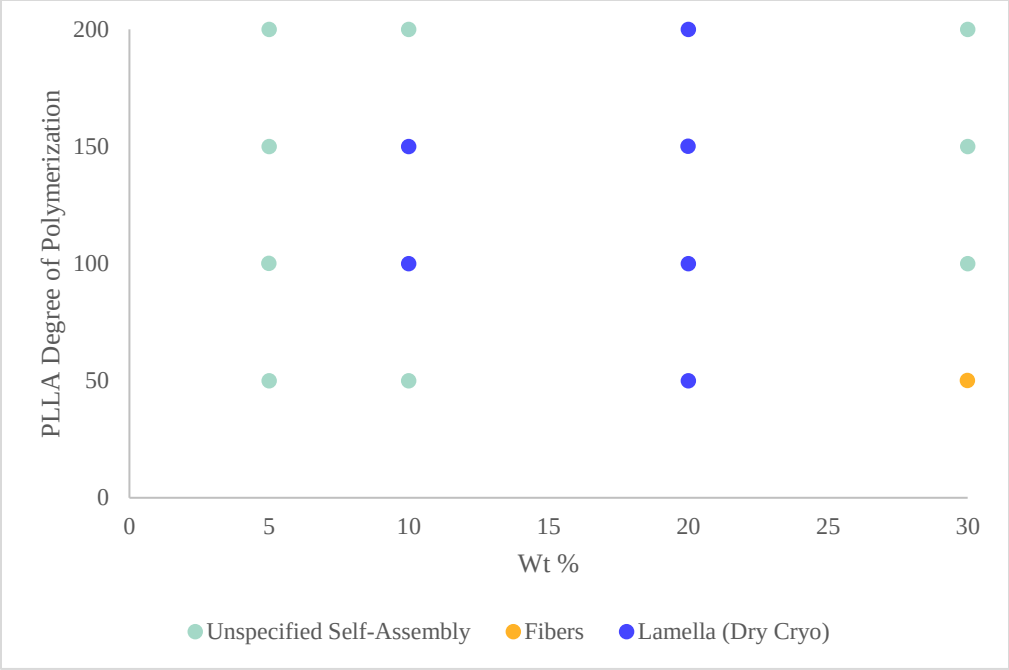

Figure 12: *The morphology of PEP_{10}-b-$PLLA_n$ self-assemblies depends on the length of the L-lactide block and the BCP concentration at the time of L-lactide polymerization.*

CONCLUSIONS

In conclusion, chlorhexidine is a pharmaceutical compound that can be used as a catalyst to polymerize L-lactide to form one-pot self-assembled nanostructures. The catalytic efficacy of chlorhexidine is comparable to DBU and TBD, but chlorhexidine also co-initiates ROP. When it is acting as an initiator, chlorhexidine is able to effectively polymerize L-lactide into homopolymers, but FTIR indicates that chlorhexidine is altered by the reaction, and MALDI-TOF indicates that chlorhexidine is not molecularly bound to the final polymer. My research could be expanded upon by determining the precise covalent binding of chlorhexidine to the PLLA homopolymers and by expanding the scope of drug catalysis by testing other pharmaceuticals which contain guanidine groups. In addition, it was successfully demonstrated that PEP can be used in place of PEG to form self-assembled nanostructures in toluene through the ROPI-CDSA process. Unlike PEG, PEP contains side chains. These can be customized with functional groups

for potential post-assembly functionalization, such as binding an azide-modified doxorubicin molecule to the polymer using a CuAAC "click" reaction.[32] Collectively these results have demonstrated the scope of ROPI-CDSA can be expanded through the development of new catalysts and solvophilic blocks. This is an important step towards the application of these materials in drug delivery.

REFERENCES

1. Sellaturay, P.; Nasser, S.; Ewan, P. Polyethylene Glycol–Induced Systemic Allergic Reactions (Anaphylaxis). *The Journal of Allergy and Clinical Immunology: In Practice* **2021**, *9* (2), 670–675.
2. Tallury, P.; Alimohammadi, N.; Kalachandra, S. Poly(Ethylene-Co-Vinyl Acetate) Copolymer Matrix for Delivery of Chlorhexidine and Acyclovir Drugs for Use in the Oral Environment: Effect of Drug Combination, Copolymer Composition and Coating on the Drug Release Rate. *Dental Materials* **2007**, *23* (4), 404–409.
3. Wen, J.; Kim, G. J. A.; Leong, K. W. Poly(d,Llactide–Co-Ethyl Ethylene Phosphate)s as New Drug Carriers. *Journal of Controlled Release* **2003**, *92* (1), 39–48.
4. Canning, S. L.; Smith, G. N.; Armes, S. P., A Critical Appraisal of RAFT-Mediated Polymerization-Induced Self-Assembly. *Macromolecules* **2016,** *49* (6), 1985-2001.
5. Qiu, H.; Du, V. A.; Winnik, M. A.; Manners, I. Branched Cylindrical Micelles via Crystallization-Driven Self-Assembly. *J. Am. Chem. Soc.* **2013**, *135* (47), 17739–17742.
6. Rupar, P. A.; Chabanne, L.; Winnik, M. A.; Manners, I. Non-Centrosymmetric Cylindrical Micelles by Unidirectional Growth. *Science* **2012**, *337* (6094), 559–562.
7. Mai, Y.; Eisenberg, A. Self-Assembly of Block Copolymers. *Chem. Soc. Rev.* **2012**, *41* (18), 5969–5985.
8. Moad, G.; Rizzardo, E.; Thang, S. H. RAFT Polymerization and Some of Its Applications. *Chemistry – An Asian Journal* **2013**, 8 (8), 1634–1644.
9. Israelachvili, J. N.; Mitchell, D. J.; Ninham, B. W. Theory of Self-Assembly of Hydrocarbon Amphiphiles into Micelles and Bilayers. *J. Chem. Soc*., Faraday Trans. 2 **1976**, 72, 1525.
10. MacFarlane, L.; Zhao, C.; Cai, J.; Qiu, H.; Manners, I. Emerging Applications for Living Crystallization-Driven Self-Assembly. Chem. Sci. 2021, 12 (13), 4661–4682.
11. Wright, D. B.; Patterson, J. P.; Gianneschi, N. C.; Chassenieux, C.; Colombani, O.; O'Reilly, R. K. Blending Block Copolymer Micelles in Solution; Obstacles of Blending. *Polym Chem* **2016**, 7 (8), 1577–1583.
12. Gao, Z.; Varshney, S. K.; Wong, S.; Eisenberg, A. Block Copolymer "Crew-Cut" Micelles in Water. *Macromolecules* **1994**, 27 (26), 7923–7927.
13. J. Derry, M.; A. Fielding, L.; P. Armes, S. Industrially-Relevant Polymerization-Induced Self-Assembly Formulations in Non-Polar Solvents: RAFT Dispersion Polymerization of Benzyl Methacrylate. *Polymer Chemistry* **2015**, 6 (16), 3054–3062.
14. Penfold, N. J. W.; Yeow, J.; Boyer, C.; Armes, S. P. Emerging Trends in Polymerization-Induced Self-Assembly. *ACS Macro Lett.* **2019**, 8 (8), 1029–1054.
15. Burridge, K. M.; Wright, T. A.; Page, R. C.; Konkolewicz, D. Photochemistry for Well-Defined Polymers in Aqueous Media: From Fundamentals to Polymer Nanoparticles to Bioconjugates. *Macromol Rapid Commun* **2018**, 39 (12), e1800093.
16. Pitto-Barry, A.; Kirby, N.; Dove, A. P.; O'Reilly, R. K. Expanding the Scope of the Crystallization-Driven Self-Assembly of Polylactide-Containing Polymers. *Polym. Chem.* **2014**, *5* (4), 1427–1436.
17. Wang, X.; Guerin, G.; Wang, H.; Wang, Y.; Manners, I.; Winnik, M. A. Cylindrical Block Copolymer Micelles and Co-Micelles of Controlled Length and Architecture. *Science* **2007**, 317 (5838), 644–647.

18. Yu, W.; Inam, M.; Jones, J. R.; Dove, A. P.; O'Reilly, R. K. Understanding the CDSA of Poly(Lactide) Containing Triblock Copolymers. *Polym. Chem.* **2017**, 8 (36), 5504–5512.
19. Hurst, P. J.; Rakowski, A. M.; Patterson, J. P. Ring-Opening Polymerization-Induced Crystallization-Driven Self-Assembly of Poly-L-Lactide-Block-Polyethylene Glycol Block Copolymers (ROPI-CDSA). *Nat Commun* **2020**, *11* (1), 4690.
20. Simón, L.; Goodman, J. M. The Mechanism of TBD-Catalyzed Ring-Opening Polymerization of Cyclic Esters. *J. Org. Chem.* **2007**, *72* (25), 9656–9662.
21. Lohmeijer, B. G. G.; Pratt, R. C.; Leibfarth, F.; Logan, J. W.; Long, D. A.; Dove, A. P.; Nederberg, F.; Choi, J.; Wade, C.; Waymouth, R. M.; Hedrick, J. L. Guanidine and Amidine Organocatalysts for Ring-Opening Polymerization of Cyclic Esters. *Macromolecules* **2006**, *39* (25), 8574–8583.
22. Bordes, C.; Fréville, V.; Ruffin, E.; Marote, P.; Gauvrit, J. Y.; Briançon, S.; Lantéri, P. Determination of Poly(ε-Caprolactone) Solubility Parameters: Application to Solvent Substitution in a Microencapsulation Process. *International Journal of Pharmaceutics* **2010**, *383* (1), 236–243.
23. Sato, S.; Gondo, D.; Wada, T.; Kanehashi, S.; Nagai, K. Effects of Various Liquid Organic Solvents on Solvent-Induced Crystallization of Amorphous Poly(Lactic Acid) Film. *Journal of Applied Polymer Science* **2013**, *129* (3), 1607–1617.
24. Discher, D. E.; Eisenberg, A. Polymer Vesicles. *Science* **2002**, *297* (5583), 967–973.
25. Clément, B.; Grignard, B.; Koole, L.; Jérôme, C.; Lecomte, P. Metal-Free Strategies for the Synthesis of Functional and Well-Defined Polyphosphoesters. *Macromolecules* **2012**, *45* (11), 4476–4486.
26. Kudo, H.; Nishioka, S.; Jin, H.; Maekawa, H.; Nakamura, S.; Masuda, T. Thermosetting Epoxy Resin System: Ring-Opening by Copolymerization of Epoxide with D,L-Lactide. *Polymer* **2022**, *240*, 124489.
27. Vilgis, T.; Halperin, A. Aggregation of coil-crystalline block copolymers: equilibrium crystallization. *Macromolecules* **1991**, 24, 2090–2095.
28. Sawinski, P. K.; Meven, M.; Englert, U.; Dronskowski, R. Single-Crystal Neutron Diffraction Study on Guanidine, CN3H5. *Crystal Growth & Design* **2013**, *13* (4), 1730–1735.
29. Zhan, S.; Wan, Z.; Zhao, Y.; Wang, J.; Li, Z. Ring-Opening Dispersion Polymerization of L-Lactide Initiated by L-Arginine in Supercritical Carbon Dioxide. *Polymer Degradation and Stability* **2020**, *171*, 109049.
30. Lim, Y. H.; Tiemann, K. M.; Heo, G. S.; Wagers, P. O.; Rezenom, Y. H.; Zhang, S.; Zhang, F.; Youngs, W. J.; Hunstad, D. A.; Wooley, K. L. Preparation and *in Vitro* Antimicrobial Activity of Silver-Bearing Degradable Polymeric Nanoparticles of Polyphosphoester- *Block* -Poly(L -Lactide). *ACS Nano* **2015**, *9* (2), 1995–2008.
31. Kamber, N. E.; Jeong, W.; Waymouth, R. M.; Pratt, R. C.; Lohmeijer, B. G. G.; Hedrick, J. L. Organocatalytic Ring-Opening Polymerization. *Chem. Rev.* **2007**, *107* (12), 5813–5840.
32. Dong, S.; Sun, Y.; Liu, J.; Li, L.; He, J.; Zhang, M.; Ni, P. Multifunctional Polymeric Prodrug with Simultaneous Conjugating Camptothecin and Doxorubicin for PH/Reduction Dual-Responsive Drug Delivery. *ACS Appl. Mater. Interfaces* **2019**, *11* (9), 8740–8748.

SUPPORTING INFORMATION

EXPERIMENTAL METHODS

Materials: L-lactide was recrystallized in toluene x3 and mPEG (Sigma Aldrich) 2000 MW was azeotropically distilled in toluene x2. Anhydrous toluene (99.8%), chlorhexidine, and 1,5,7 triazabicyclodec-5-ene were purchased from Sigma Aldrich without further purification. Poly-2-ethoxy-2-oxo-1,3,2-dioxaphospholane was purchased from TCI Chemicals without further purification. Benzoic acid was purchased from Fisher Chemical without further purification. All chemicals were stored, and all reactions were performed under N_2 in a glovebox.

Characterization Methods: ^{1}H Nuclear Magnetic Resonance (^{1}H NMR) spectra were collected using a 500 MHz Bruker DRX500 spectrometer equipped with a cryoprobe. All samples were dissolved in $CDCl_3$, and all shifts were taken in ppm, calibrated to a TMS standard. % conversion was calculated using Equation 1. Gel permeation chromatography (GPC) measurements were taken using an Agilent 1100 chromatograph with a PL gel 5 μm 300x7.5mm mixed-column and a RID detector. The samples were dissolved and run in DMF. Cryo-transmission electron microscopy (cryo-TEM) samples were prepared from extracted solutions and blotted onto Quantifoil grids using a Leica cryo-Plunger. The grids were blotted for 3s and plunged into liquid propane. The grids were imaged using a JOEL 2100F microscope with a OneView camera on a Gatan Cryo-TEM holder. All analysis instruments were located at the University of California in Irvine.

Polymer Synthesis

Supplementary Scheme 1: DBU catalyzed ROP of PEG-*b*-PLLA

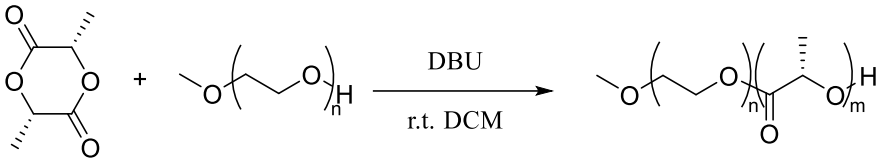

DBU catalyzed ROP: DBU (0.1 mol%) and mPEG were dissolved in DCM (0.425 M L-LA) in a glovebox at r.t. The solution was then added to L-lactide and allowed to stir for 20 minutes. The mixture was then quenched with 5 mg of benzoic acid via a saturated benzoic acid solution in toluene. The ratio of mPEG to L-lactide was varied to yield the Target DPs in Table 1. ^{1}H NMR of the crude was taken in $CDCl_3$ to determine the % conversion. ^{1}H NMR (499 MHz, $CDCl_3$) δ 7.26 (s, 75 H $CDCl_3$), 5.30 (s, 1051 H DCM), 5.17 (q, 40 H), 5.03 (q, 0.5 H), 3.64 (s, 180 H), 1.57 (m, 228 H), 1.27 (b, 206 H), 0.89 (m, 48 H). ^{1}H NMR of the purified was taken in $CDCl_3$ to determine the degree of polymerization . ^{1}H NMR (499 MHz, $CDCl_3$) δ 7.26 (s, 35 H $CDCl_3$), 5.22 (m, 49 H), 3.70 (s, 180 H), 3.54 (q, J = 7 Hz, 35 H), 3.43 (s, 3 H), 1.69 (b, 103 H), 1.62 (m, 156 H), 1.26 (t, J = 14, 47 H).

Supplementary Scheme 2: Chlorhexidine catalyzed ROP of PEG-*b*-PLLA

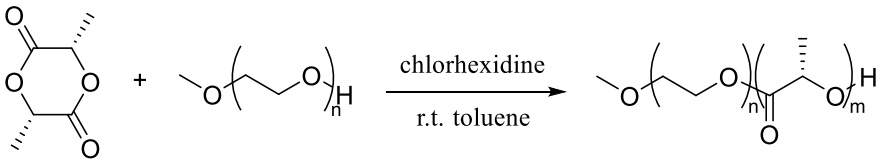

Chlorhexidine (5 mol%) was was mixed with toluene to form a colloidal solution. mPEG was added to the colloidal solution, then the solution was added to L-lactide once the mPEG had dissolved. The solution was allowed to stir for 30 minutes before the reaction was quenched with 0.05 mL of a saturated benzoic acid solution in toluene. The ratio of mPEG to L-lactide was varied to yield the Target DPs in Table 1. ^{1}H NMR of the crude was taken in $CDCl_3$ to determine the % conversion and the degree of polymerization. ^{1}H NMR (499 MHz, $CDCl_3$) δ 7.23 (m, toluene),

7.18 (m, toluene), 5.17 (q, J = 7 Hz, 88 H), 5.03 (m, 1 H), 4.36 (q, J = 7 Hz, 5 H), 3.64 (s, 180 H), 3.38 (s, 5 H), 2.35 (s, 25 H) 1.58 (m, 282 H).

Supplementary Scheme 3: Chlorhexidine catalyzed and initiated ROP of PLLA

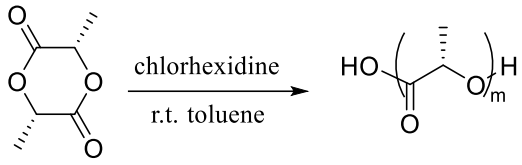

Chlorhexidine (5 mol%) was was mixed with toluene to form a colloidal solution. m_2PEG was added to the colloidal solution, then the solution was added to L-lactide once the m_2PEG had dissolved. The solution was allowed to stir for 30 minutes before the reaction was quenched with 0.05 mL of a saturated benzoic acid solution in toluene. The ratio of m_2PEG to L-lactide was varied to yield the Target DPs in Table 2 for easy comparison to the reactions in Table 1, even though m_2PEG is not an initiator in this reaction. ^{1}H NMR of the crude was taken in $CDCl_3$ to determine the % conversion. ^{1}H NMR (499 MHz, $CDCl_3$) δ 7.39 (m, toluene), 7.38 (m, toluene), 5.39 (m, 59 H), 4.93 (q, J = 6 Hz, 18 H), 3.86 (s, 180 H), 2.57 (toluene), 1.80 (m, 262 H).

Supplementary Scheme 4: TBD catalyzed and initiated ROP of PLLA

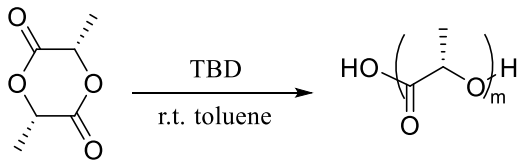

L-lactide and m_2PEG were dissolved in toluene and stirred at 400 rpm. The ratio of m_2PEG to L-lactide was varied to yield the Target DPs in Table 3, if m_2PEG had been an initiator. TBD (0.1 mol%) was added from a toluene stock solution (4.3 mg/mL) and ethanol (if applicable) was added to yield the Target DPs in Table 3. The solution was allowed to stir for 90 seconds before the reaction was quenched with 0.05 mL of a saturated benzoic acid solution in toluene. ^{1}H NMR of the crude was taken in $CDCl_3$ to determine the % conversion. ^{1}H NMR (499 MHz, $CDCl_3$) δ 7.26

(m, toluene), 7.18 (m, toluene), 5.17 (q, J = 7 Hz, 94 H), 5.03 (q, J = 7 Hz, 4 H), 3.64 (s, 180 H), 3.37 (s, 6 H), 2.35 (toluene), 1.58 (d, J = 7 Hz, 276 H).

Supplementary Scheme 5: TBD catalyzed and initiated ROP of PEP-*b*-PLLA

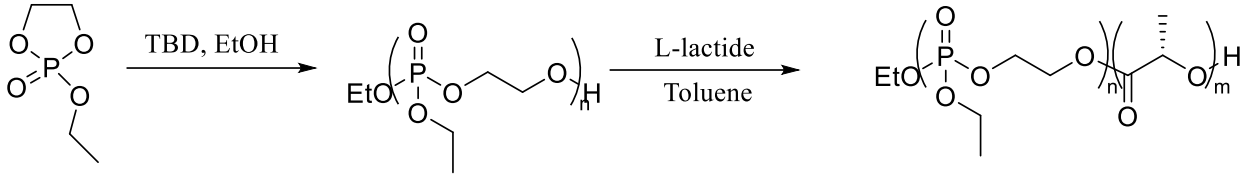

2-Ethoxy-2-oxo-1,3,2-dioxaphospholane, TBD (1 mol%), and ethanol were stirred neat at room temperature for 20 minutes. The ratio of ethanol to poly-2-ethoxy-2-oxo-1,3,2-dioxaphospholane was varied to change the DP of PEP. L-lactide was dissolved in toluene and added to the solution. The ratio of ethanol to L-lactide was varied to change the degree of polymerization, and the volume of toluene was varied to control the concentration of the BCP during self-assembly. The combined solution was stirred for 90 seconds and quenched with 0.05 mL of benzoic acid solution in toluene. ^{1}H NMR of the crude was taken in $CDCl_3$ to determine the % conversion. ^{1}H NMR (499 MHz, $CDCl_3$) δ 7.21 (m, toluene), 7.14 (m, toluene), 5.14 (q, J = 7 Hz, 140 H), 4.63 (q, J = 6 Hz, 5 H), 4.09 (m, 42 H), 2.31 (toluene), 1.56 (d, J = 7 Hz, 395 H), 1.30 (q, J = 7 Hz, 25 H).

Supplementary Scheme 6: DBU catalyzed and initiated ROP of PEP-*b*-PLLA

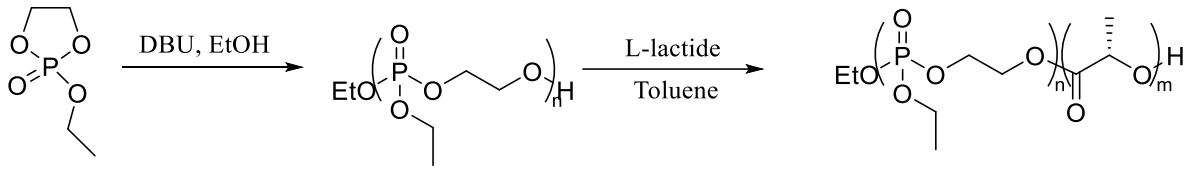

2-Ethoxy-2-oxo-1,3,2-dioxaphospholane, DBU (5 mol%), and ethanol were stirred neat at room temperature for 7 minutes. The ratio of ethanol to poly-2-ethoxy-2-oxo-1,3,2-dioxaphospholane was varied to change the DP of PEP. L-lactide was dissolved in toluene and added to the solution. The ratio of ethanol to L-lactide was varied to change the degree of polymerization, and the volume

of toluene was varied to control the concentration of the BCP during self-assembly. The combined solution was stirred for 4 minutes until the L-lactide completely dissolved and quenched with 0.05 mL of benzoic acid solution in toluene. ^{1}H NMR of the crude was taken in $CDCl_3$ to determine the % conversion. ^{1}H NMR of the crude was taken in $CDCl_3$ to determine the % conversion. ^{1}H NMR (499 MHz, $CDCl_3$) δ 7.26 (m, toluene), 7.18 (m, toluene), 5.17 (q, J = 7 Hz, 96 H), 4.82 (q, J = 6 Hz, 4 H), 4.25 (s, 32 H), 4.16 (m, J = 7 Hz, 21 H), 2.35 (toluene), 1.59 (d, J = 7 Hz, 285 H), 1.36 (q, J = 7 Hz, 30 H).

Supplementary Scheme 7: DBU catalyzed and initiated ROP of PEP

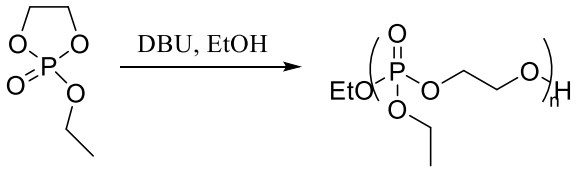

2-Ethoxy-2-oxo-1,3,2-dioxaphospholane, DBU (5 mol%), and ethanol were stirred neat at room temperature for 7 minutes. The ratio of ethanol to poly-2-ethoxy-2-oxo-1,3,2-dioxaphospholane was varied to change the DP of PEP. The solution was then quenched with 0.05 mL of benzoic acid solution in toluene. ^{1}H NMR of the crude was taken in $CDCl_3$ to determine the % conversion. ^{1}H NMR (499 MHz, $CDCl_3$) δ 7.26 (m, toluene), 7.19 (m, toluene), 4.26 (s, 20 H), 4.17 (m, J = 7 Hz, 15 H), 2.36 (toluene), 1.36 (t, J = 7 Hz, 20 H).

BCP purification in cold diethyl ether

The toluene was evaporated from the crude BCP mixture, then it was dissolved in a small amount chloroform to form a saturated solution. The chloroform solution was dropped into 200 mL of diethyl ether (90%) and methanol (10%) chilled in a dry ice and isopropyl alcohol bath. The polymers precipitated from the diethyl ether as long white waxy strands, which were collected with a filter.

SUPPLEMENTARY TABLES AND FIGURES

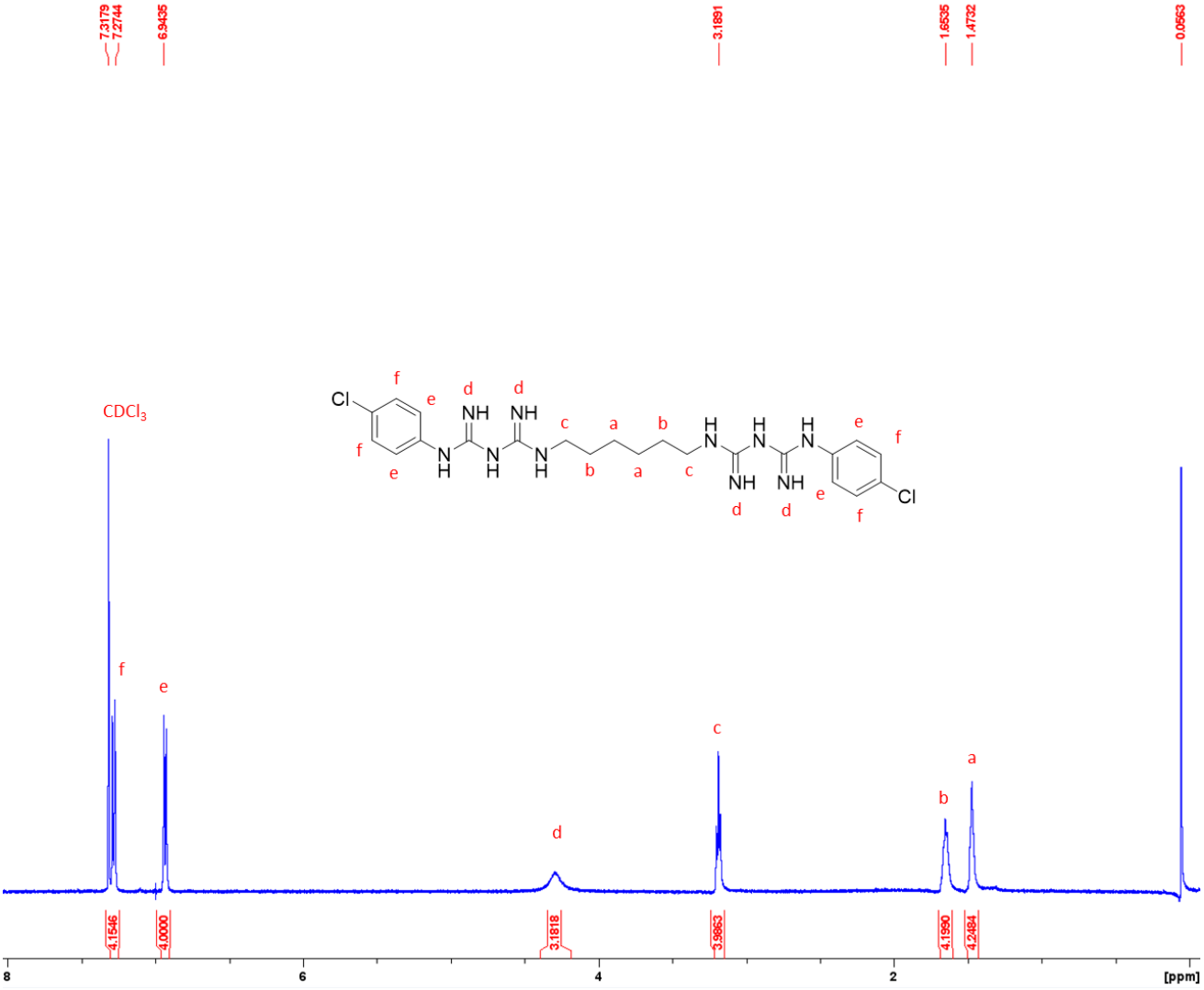

Figure S 1: *H NMR spectra for chlorhexidine for identification of chlorhexidine peaks in crude NMRs post-ROP*

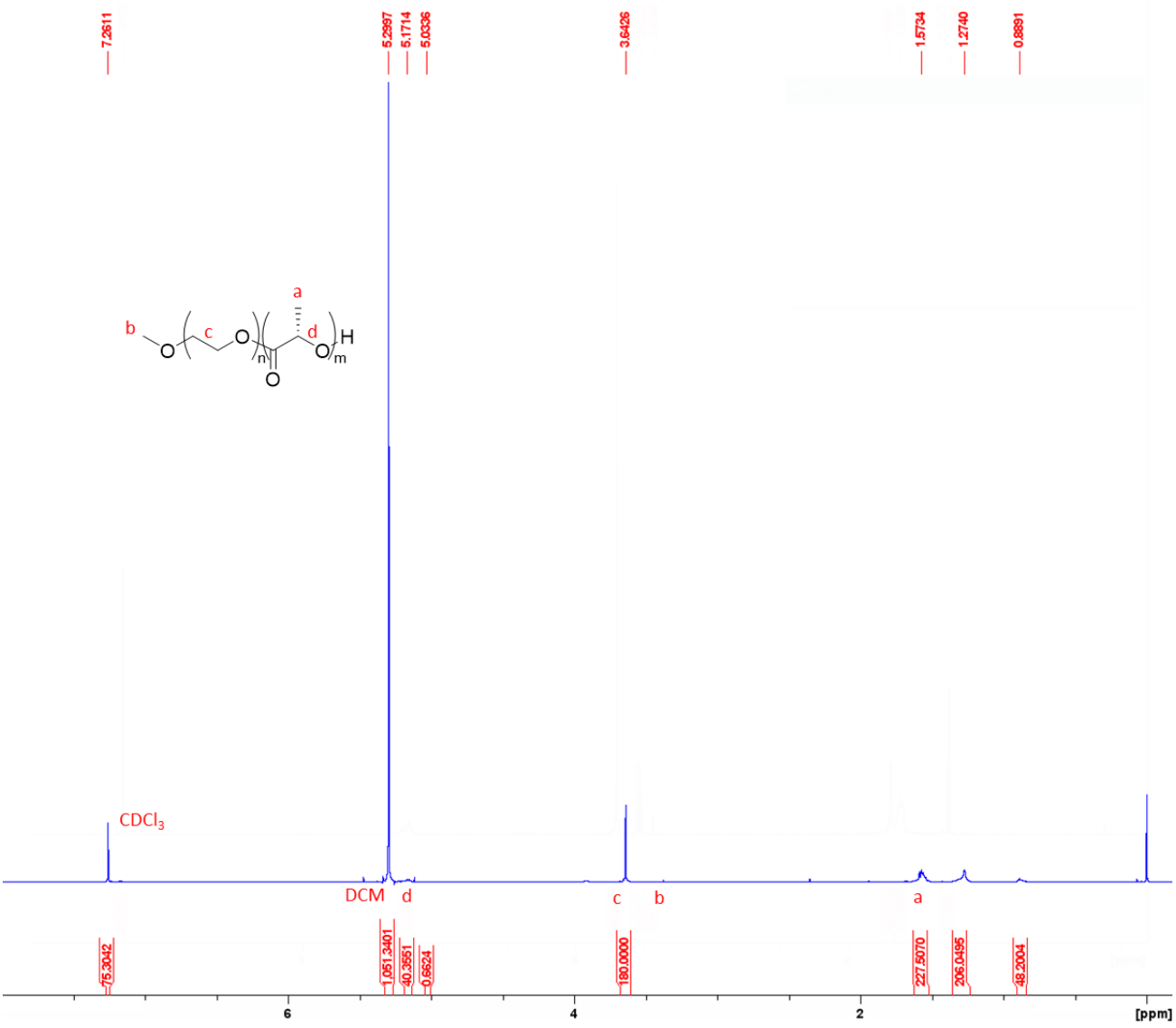

Figure S 2: *crude H NMR of* PEG-*b*-PLLA *synthesized using DBU. This H NMR is used to calculate the percent conversion.*

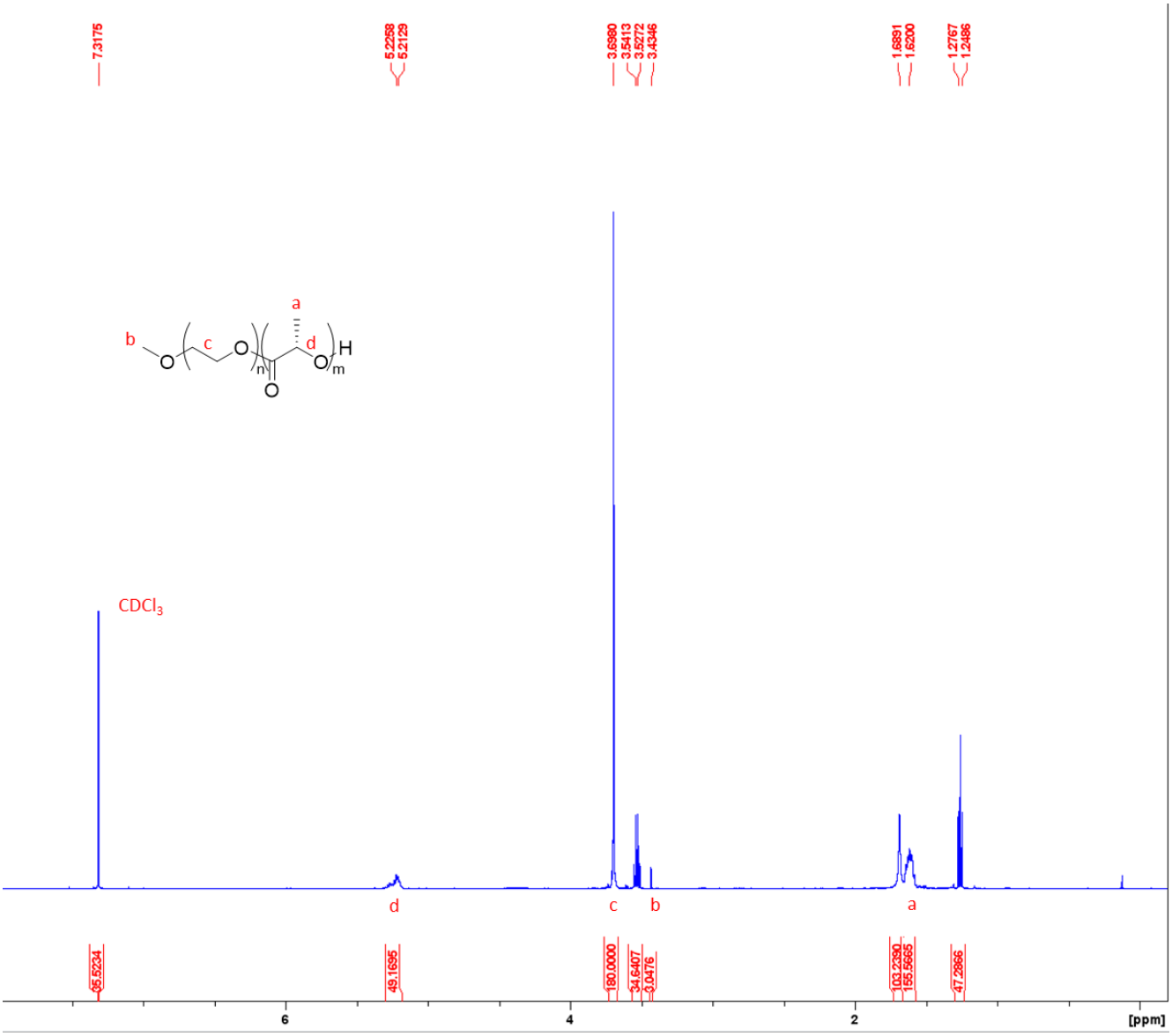

Figure S 3: *H NMR of* PEG-*b*-PLLA *synthesized using DBU, after purification. This H NMR is used to calculate the degree of polymerization.*

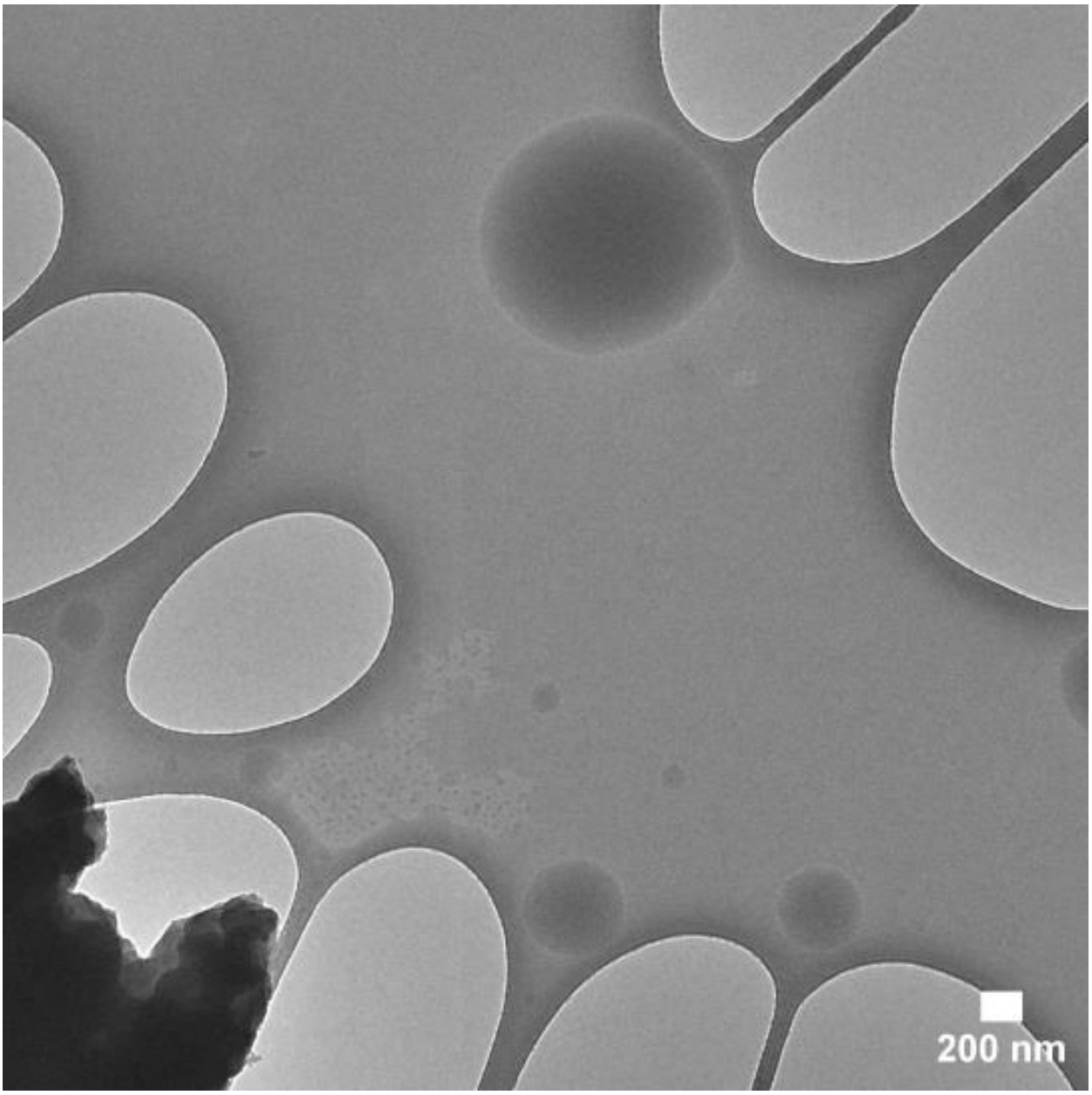

Figure S 4: *Lamellae aggregate (bottom left) and circular features in dry cryoTEM image of PEP_{10}-b-$PLLA_{50}$, self-assembled at 20% wt.*

$$\%\ Conversion = \frac{Integration\ of\ PLLA\ peak\ at\ 5.2}{Integration\ of\ PLLA\ peak\ at\ 5.2 + Integration\ of\ PLLA\ peak\ at\ 5.0} * 100\%$$

Equation 1: This equation is used to calculate the % conversion of PLLA

$$Degree\ of\ Polymerization = \frac{Integration\ of\ PLLA\ peak\ at\ 5.2}{Integration\ of\ mPEG\ peak\ at\ 3.6} * 180$$

Equation 2: This equation is used to calculate the degree of polymerization of PLLA

Table S1: Full characterization list of PEP-*b*-PLLA BCPs in toluene

PEP DP	PLLA DP	Wt %	Turbid?	% Conversion	Đ
10	50	5	Y	98.6	2.31
10	100	5	Y	95.0	1.33
10	150	5	Y	99.9	1.36
10	200	5	Y	99.8	-
10	50	10	Y	91.1	-
10	100	10	Y	93.0	1.31
10	150	10	Y	99.9	-
10	200	10	Y	99.7	-
10	50	20	Y	98.3	1.54
10	100	20	Y	95.6	1.19
10	150	20	Y	97.2	1.25
10	200	20	Y	97.9	1.27
10	50	30	Y	96.5	1.17
10	100	30	Y	98.9	1.47
10	150	30	Y	99.0	1.56
10	200	30	Y	98.2	-
20	50	5	N	-	-
20	100	5	N	-	-
20	150	5	N	-	-
20	100	5	N	-	-
20	50	10	N	98.7	-
20	100	10	Y	-	-
20	150	10	Y	98.3	-
20	200	10	Y	99.7	-
20	50	20	Y	90.9	1.70
20	100	20	Y	95.2	1.45
20	150	20	Y	95.8	1.38
20	200	20	Y	99.9	-
20	50	30	Y	-	-
20	100	30	Y	-	-
20	150	30	Y	-	-
20	200	30	Y	-	-

*Data incomplete due to ^{1}H NMR and GPC malfunctions and limitations of the GPC spectrometer